Check for updates

Identification of subsurface archaeology at Mutaredh, United Arab Emirates, using ground penetrating radar

Sonia Santos-Assunção[1], Moamen Ali[1], Mohammed Y. Ali[1], Diana Francis[1,2]*, Peter Sheehan[3], Waleed Awad Omar[3] and Muhammad Asim Iqbal[1]

[1]Department of Earth Sciences, Khalifa University of Science and Technology, Abu Dhabi, United Arab Emirates, [2]Environmental and Geophysical Sciences (ENGEOS) Lab, Khalifa University of Science and Technology, Abu Dhabi, United Arab Emirates, [3]Department of Culture and Tourism, Abu Dhabi, United Arab Emirates

The United Arab Emirates holds great historical importance, as evidenced by many archaeological sites, such as the Jebel Hafit Tombs and the Hili Archeological Park in Al Ain. At the western edge of Mutaredh Oasis, a major new archaeological site was discovered in 2023 during a construction project. Several important archeological features have been documented, including an earthen mosque and boundary walls, Iron Age irrigation systems, and a circular stone tomb dating to the Bronze Age. However, the eastern edge of the Mutaredh site has remained unexplored to date. Ground Penetrating Radar (GPR) has been proven to be a successful method in mapping archaeological remains. Accordingly, a high-resolution GPR survey was carried out to identify the continuity of the unearthed archeological elements and delineate new unexplored features. A comprehensive 3D model of buried archaeological features was constructed using the acquired high-resolution GPR data in the eastern part of the Mutaredh site. Several selected anomalies have been observed, similar to the uncovered features in the western part of the Mutaredh site and structures documented in other nearby archaeological sites. The geometry and extension of these anomalies have enabled the possible identification of a further two Bronze Age circular tombs, as well as the delineation of a system of water channels (*falaj*), and irrigation networks with tree pits from the Iron Age. Moreover, walls probably belonging to the Late Islamic Age are identified. These findings suggest that Mutaredh has been a site of intensive human activity from the Bronze Age through to the Late Islamic period. Given the density of identified anomalies, further significant features are anticipated to lie buried in the immediate surrounding areas, promising continued insights into the area's rich archaeological heritage. The findings of this study may guide archaeologists to specific locations and assist in selecting the most appropriate excavation techniques for the verification stage.

KEYWORDS

archaeology, ground penetrating radar, 3D model, Bronze Age, iron age, late islamic period, UAE

1 Introduction

Geophysical methods are crucial for subsurface studies, providing non-invasive techniques to explore and characterize the Earth's interior. These methods include seismic, gravity, magnetic, electrical resistivity tomography (ERT), and ground-penetrating radar (GPR) (e.g., Telford et al., 1990; Daniels, 2004; Reynolds, 2011; Hinze et al., 2013). Geophysical techniques enable researchers to acquire valuable data about subsurface structures and stratigraphy. For instance, seismic methods are widely used for imaging subsurface layers, identifying potential oil and gas reservoirs, and monitoring CO_2 injection sites (Telford et al., 1990; Kearey et al., 2002). Magnetic and gravity methods are commonly applied to map large-scale structural features, such as sedimentary basins, salt domes, and faults, and to identify buried ore bodies (Telford et al., 1990; Kearey et al., 2002). GPR and ERT are frequently employed in near-surface studies, particularly for detecting buried archaeological features and assessing groundwater systems (e.g., Daniels, 2004; Jol, 2008; Reynolds, 2011; Conyers, 2023). By integrating geophysical data, geoscientists can more effectively identify natural resources, monitor environmental hazards, and contribute to archaeological discoveries, thus offering a comprehensive understanding of subsurface conditions.

Traditional methods of identifying potential ancient settlements through visual inspection and excavation often prove inconclusive and insufficient (Hey, 2006; White, 2013). This challenge is particularly pronounced over extensive regions completely covered by sand, where there are no visible indications of previous settlements, making it tricky to select potential areas (Schiffer et al., 1978; McManamon, 1984). Moreover, excavating without prior knowledge of the depth and size of buried elements can lead to the improper selection of tools, posing a hazard and risking the damage or destruction of valuable remnants (Bullock, 2013). In addressing these challenges, remote sensing plays a crucial role in archaeological investigations, particularly GPR, ERT, and magnetic methods (Parcak, 2007; Gaffney, 2008; Parcak, et al., 2016; Ben-Romdhane, et al., 2023). They are both non-destructive and time-efficient. The data obtained through these methods aids in determining the geometry and enables the creation of a 3D model of buried elements before excavating. This capability allows researchers to visualize the previously unseen and protect the invisible features of archaeological sites (Nuzzo, et al., 2002; Palumbo, et al., 2014; El-Qady et al., 2019).

GPR provides high-resolution data for shallow environments with low or no salt and clay content (Daniels, 2000; Annan, 2009). GPR has proven successful when used independently or in conjunction with other geophysical techniques to survey potential archaeological sites (Neubauer et al., 2002; Trinks et al., 2010; Pérez-Gracia et al., 2012; Conyers, 2015; Assunção et al., 2018). For a comprehensive understanding of GPR procedures in archaeology, one can refer to works such as Conyers (2007), and more recently, Goodman and Piro (2013), Conyers (2023), Goodman and Piro (2013), and Conyers (2023). High-frequency GPR antennas have proven effective in determining structural arrangements and tracing pathologies, as demonstrated in a Beehive Mycenae tomb study in Greece (Roumelioti, 2022; Santos-Assunçao et al., 2016). Several circular tombs were accurately investigated using GPR, including the Nutubaru burial mound in Miyazaki under a forest in Japan
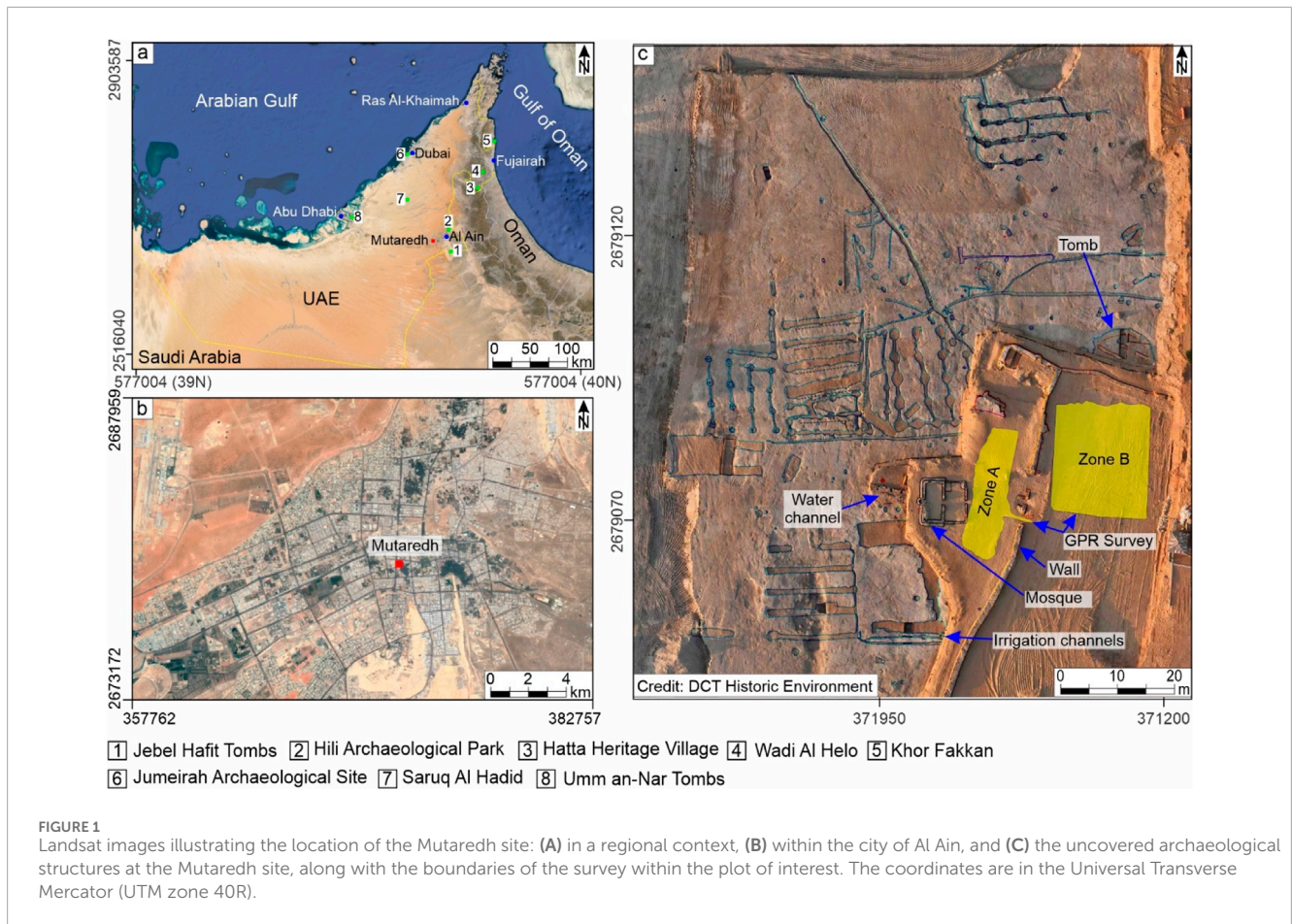
(Dean et al., 2004) and multiple tombs in a snow-covered field in Norway (Gabler et al., 2019). Büyüksaraç, Yalçıner et al. (2014) conducted geophysical investigations integrating GPR, Electrical Resistivity Tomography (ERT), and Magnetic Imaging (MI) to detect traces of cemeteries. Similarly, Koşaroğlu et al. (2022) employed only GPR to map historical graves successfully.

The United Arab Emirates (UAE) became a country in 1971, uniting seven Emirates (Abu Dhabi, Dubai, Sharjah, Ajman, Um Al Qwain, Ras Al-Khaimah and Fujairah). Archaeological evidence suggests that this region has been inhabited for over 125,000 years. Human settlements likely began in the Paleolithic period, with early Bedouin nomads traveling through the region (Potts, 1993; Tikiriti, 2002). The first archaeological excavations, started by a Danish archaeology team in 1959, uncovered significant buildings and circular tombs erected by the Umm an-Nar culture on the Island of Um an-Nar in Abu Dhabi (2,600–2,000 BCE; Figure 1A). This culture was named after its first discovery on Umm an-Nar island (UTM coordinates 247854.04 m E, 2705036.80 m N, in zone 40R), in Abu Dhabi (Frifelt et al., 1991). The circular tombs range in diameter from 6 to 12 m and stand a few meters high. These tombs consist of multiple chambers accessed through narrow entrances and were designed to accommodate several bodies (Madsen, 2018). Similar structures were excavated in nearby regions in the UAE and Oman.

Approximately 130 km to the east of Umm an-Nar Island, near the border with Oman, the mountain of Jebel Hafit lies to the south of Al Ain City, rising 1,000 m above the surrounding plain. The early inhabitants of Al Ain region selected the northern and eastern slopes of Jebel Hafit to build a series of tombs for their deceased. Each domed tomb features a single round or oval chamber, measuring about 2–3 m in width, constructed from local rocks in an uncut or rough-cut manner. Encircling the chamber are ring walls that reach a height of 3–4 m. The Jebel Hafit tombs, characterized by narrow entrances, housed the remains and belongings of two to five people (Madsen, 2018). This is in contrast to the later Umm an-Nar tombs, where hundreds of people were buried together over long periods (Frifelt et al., 1991; Belmonte and González-García, 2014). The geological composition of Jebel Hafit, the nearby mountain, comprises shallow marine sedimentary rocks, including limestone, evaporites, and marl (Ali et al., 2008; Ullah et al., 2023). The citizens of Al Ain used to utilize local stones for construction and tool production (Swerida, 2018). Therefore, it is expected to find limestone as a constructive material type embedded in the reddish dry sand (Cherif et al., 1992; Warrak, 1996).

Moreover, in the UAE, numerous archaeological sites, such as Hili Archaeological Park, Bida Bint Saud, Baynunah Fossil Site, Jumeirah Archaeological Site, Hatta Heritage Village, Wadi Al Helo, Khor Fakkan, Al Thuqaibah, Sieh Al Herf and Necropolis of Shimal, underscore the rich historical heritage of the country (Yagoub and Al Yammahi, 2022; Potts, 2012). Importantly, these sites are protected by specific rules to preserve their historical and cultural significance (Alnimee, 2020).

In Al Ain, structures dating back to both the Bronze Age (3200 BCE to 1300 BCE) and Iron Age (1300 BCE to 300 BCE) have been documented, revealing various purposes such as residences, protective towers, water wells, and circular tombs (Jorgensen and al-Tikiriti, 2003; Power and Sheehan, 2012; Tikriti, 2002; Al-Tikriti, 2015; Sheehan et al., 2015). Among the numerous items uncovered in Al Ain are ceramic vessels, copper relics, weapons,

FIGURE 1
Landsat images illustrating the location of the Mutaredh site: **(A)** in a regional context, **(B)** within the city of Al Ain, and **(C)** the uncovered archaeological structures at the Mutaredh site, along with the boundaries of the survey within the plot of interest. The coordinates are in the Universal Transverse Mercator (UTM zone 40R).

jewelry, and day-to-day tools (Potts, 1993; Cleuziou, 2003; Power and Sheehan, 2012; Sheehan et al., 2015; Power et al., 2019). These prehistoric buildings and features are typically located in deeper layers, and are sometimes found buried beneath later features associated with the Late Pre-Islamic period (300 BCE to 300 CE) or the Islamic period starting from 630 CE (Kim and Heliyer, 2003; Power et al., 2019; Al Marzooqi et al., 2024).
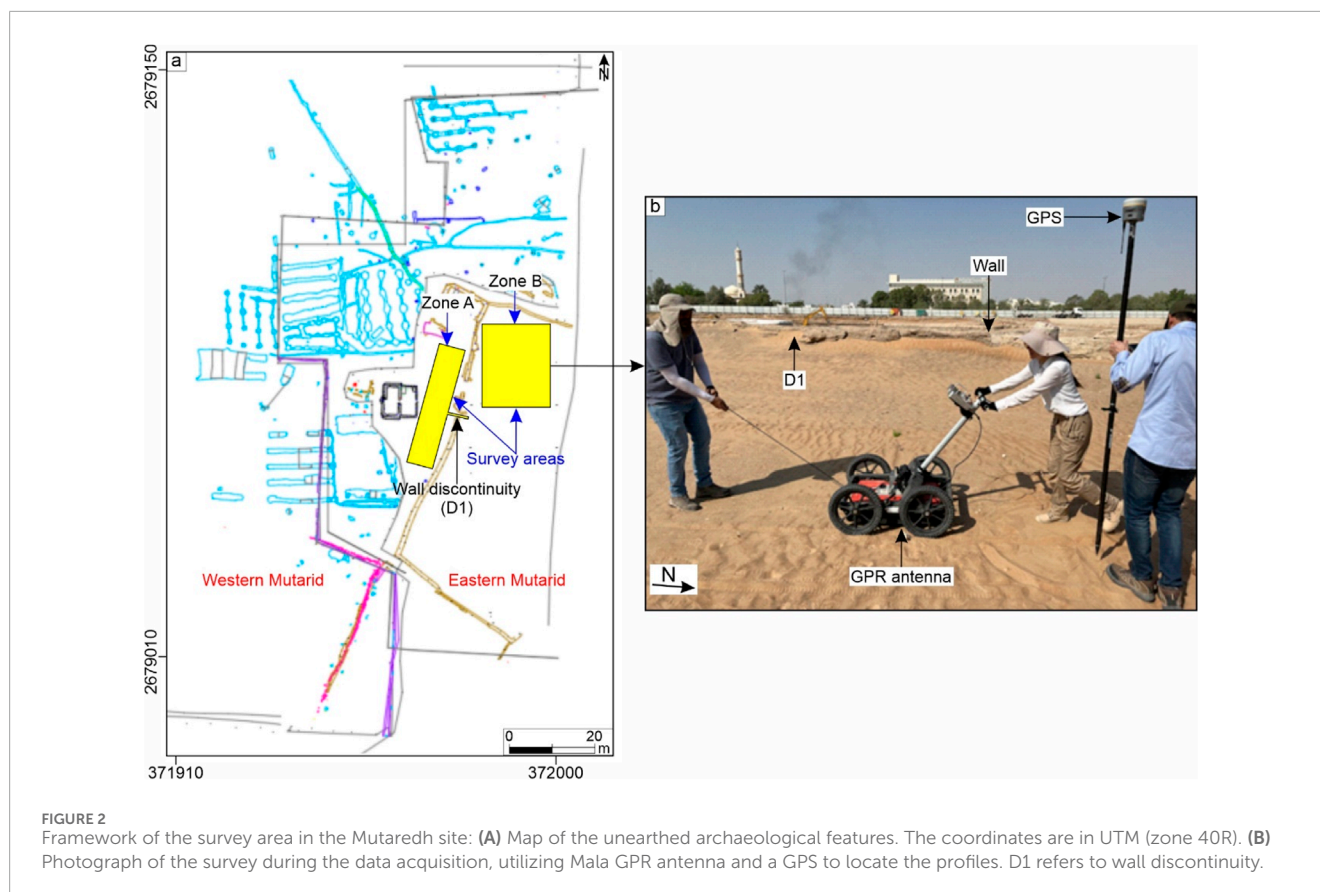
Various tools and goods discovered in the archaeological findings in the UAE have origins that can be traced to Europe and Asia, while other products from Southeast Arabia were exported to these distant regions (James Blackman et al., 1989; Belmonte and González-García, 2014). This illustrates the significance and value of maritime trade across the Arabian Gulf (Carter, 1997; Cleuziou, 2003; Strutt et al., 2013; Suryanarayan et al., 2022). Referred to as Magan in ancient times, the UAE and Oman region served as a remarkable metallurgic center (Böhme and Al-Sabri, 2011; Giardino, 2017).

The UAE and Oman region inhabitants developed settlements featuring an advanced underground water distribution network. These channels, known as *aflaj* (Arabic: sing. *falaj*), were designed to transport this vital resource over long distances (Tikriti, 2002; Wilkinson, 2002). The *aflaj* are sometimes buried a few meters below the surface and accessed via vertical holes or shafts, while in other areas, they are exposed at ground level (MRMEWR, 2011). This ancient yet efficient system is still partially in use in the UAE and Oman today (Brook and Al Houqani, 2006; Caratelli et al., 2019;

Alsharhan and Rizk 2020). These ancient systems have provided continuous water access, enabling the areas under cultivation for agricultural purposes to expand (Brook and Al Houqani, 2006; Caratelli et al., 2019; Alsharhan and Rizk, 2020).

Large red sand dunes are visible surrounding the cultivated area of the city. These dunes are shaped by strong winds and are constantly subject to erosion. Depending on the intensity and continuity of the winds, they may exert additional load on the archaeological structures, both in a short or long time (Raffaele and Bruno, 2019; Fahmy et al., 2023). The natural dynamic of the sand dunes can quickly cover and hide any archaeological evidence of the past (Raffaele and Bruno, 2019; Barbaro et al., 2022).

GPR has been successfully applied to map archaeological remains across various emirates, particularly in the Emirates of Dubai, Sharjah, and Abu Dhabi (Al Ain area). In the Emirate of Sharjah, a 3D model successfully imaged buried features from the Iron Age, revealing valuable insights into society stratum during the same age (Evangelista et al., 2002). GPR was also integrated with geomatics techniques by integrating the topographic data with subsurface results (Al-Ruzouq, Abu Dabous et al., 2022). Additionally, Carbó et al. (2000) presented a GPR study conducted in Al Madam, Sharjah, providing an evocative account of life during the Iron Age. In Saruq Al-Hadid, a renowned archaeological site in the scenic Dubai desert, a GPR survey utilizing a monostatic 270 MHz antenna was performed by Herrmann (2013) to assess the presence of archaeological remains. The results identified a prominent circular

FIGURE 2
Framework of the survey area in the Mutaredh site: **(A)** Map of the unearthed archaeological features. The coordinates are in UTM (zone 40R). **(B)** Photograph of the survey during the data acquisition, utilizing Mala GPR antenna and a GPS to locate the profiles. D1 refers to wall discontinuity.
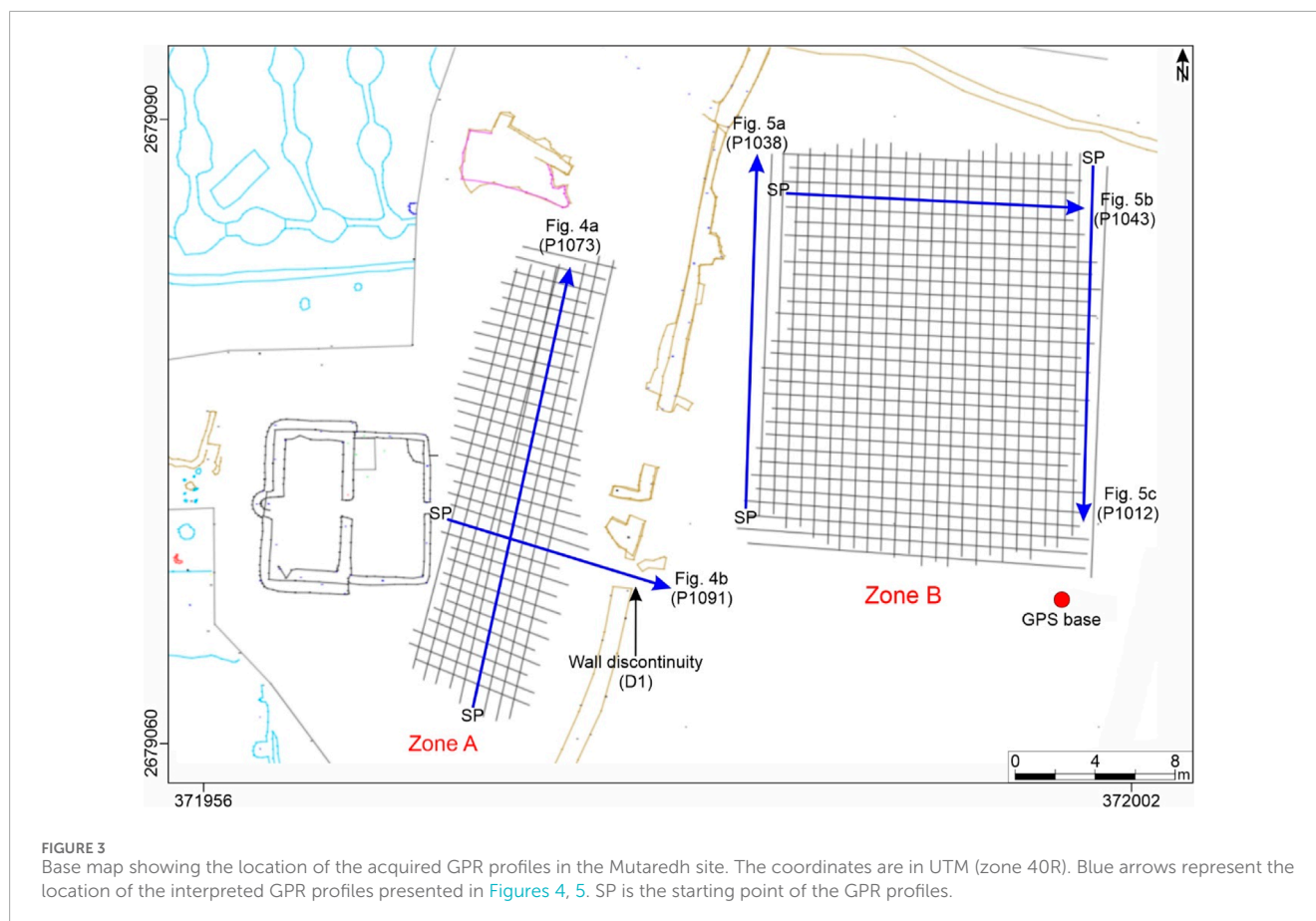
structure and other elements associated with both the Iron Age and the Wadi Suq Period, 2,000 to 1,300 BCE (Carter, 1997; Herrmann, 2013). A GPR survey in Al Ain revealed a linear anomaly, suggesting the presence of a 90 m long channel of a *falaj* system associated with the Bronze Age and Iron Age (Al Tikriti et al., 2013). The depth of this open irrigation channel, as determined by the GPR survey, varies from 1.3 to 1.8 m, depending on the location. During 2023, archaeological monitoring of excavations for a large construction project in the Mutaredh area of Al Ain (Figures 1B, C) revealed a multi-period archaeological landscape.

The excavations in the western part of the site revealed significant features from the Bronze Age, Iron Age, and Islamic periods. These archaeological structures include walls, a mosque, a circular stone tomb, a *falaj*, and agricultural irrigation systems, all built above a gravel layer. Beneath this gravel lies a very hard bedrock at a depth of approximately 2.5 m (Sheehan, in press). While the eastern section of the Mutaredh archaeological site remains unexplored to date. Therefore, the main aim of this study is to acquire and interpret high-resolution GPR data to evaluate the continuity of the archeological features already uncovered in western Mutaredh and assess the yet-unexplored eastern part of the Mutaredh archeological site. The interpretation of the anomalies will be based on pattern recognition, comparing them to archaeological features identified in the surrounding area. By creating a 3D model of the buried elements, we can precisely select the most suitable tools for excavation, significantly reducing the risk of damaging valuable elements.

2 Material and methods

A GPR survey using a mesh-type approach was acquired at the eastern Mutaredh site to assess the continuity of the anomalies along parallel profiles (Figures 1C, 2). A total of 99 GPR profiles covered the area of interest (Figure 3), with an average spacing of 0.50 m between consecutive profiles with the acquisition settings listed in Table 1. The location of each GPR profile and the site topography were determined using a differential GPS (Trimble TSC5 Controller and Trimble R12 GNSS). The GPR equipment employed an ultra-wide range Mala antenna operating within a frequency band of 80–950 MHz. In this survey, each trace has 1,001 samples with a 209 ns time window. The distance interval between two consecutive traces was 0.017 m to accurately depict the geometry of the anomalies and easily associate them with known archaeological structures. The antenna separation of 0.23 m, particularly for this system, is a fixed parameter and is correlated with the operating frequency.

The surveyed area is divided into Zone A and Zone B (Figure 3), both appearing smooth and nearly flat, as shown in Figure 2B. This division is attributed to the presence of an unearthed wall (Figures 2, 3). The elevation of the sites is 245 m above sea level. Analysis of the acquired topography data reveals a slight oscillation of only 11 cm between the minimum and maximum altitude values. The excavation data obtained from the site (Figure 2A) will be used to verify and calibrate the results of the GPR.

FIGURE 3
Base map showing the location of the acquired GPR profiles in the Mutaredh site. The coordinates are in UTM (zone 40R). Blue arrows represent the location of the interpreted GPR profiles presented in Figures 4, 5. SP is the starting point of the GPR profiles.

TABLE 1 Acquisition settings of the GPR survey conducted at the Mutaredh archeological site.

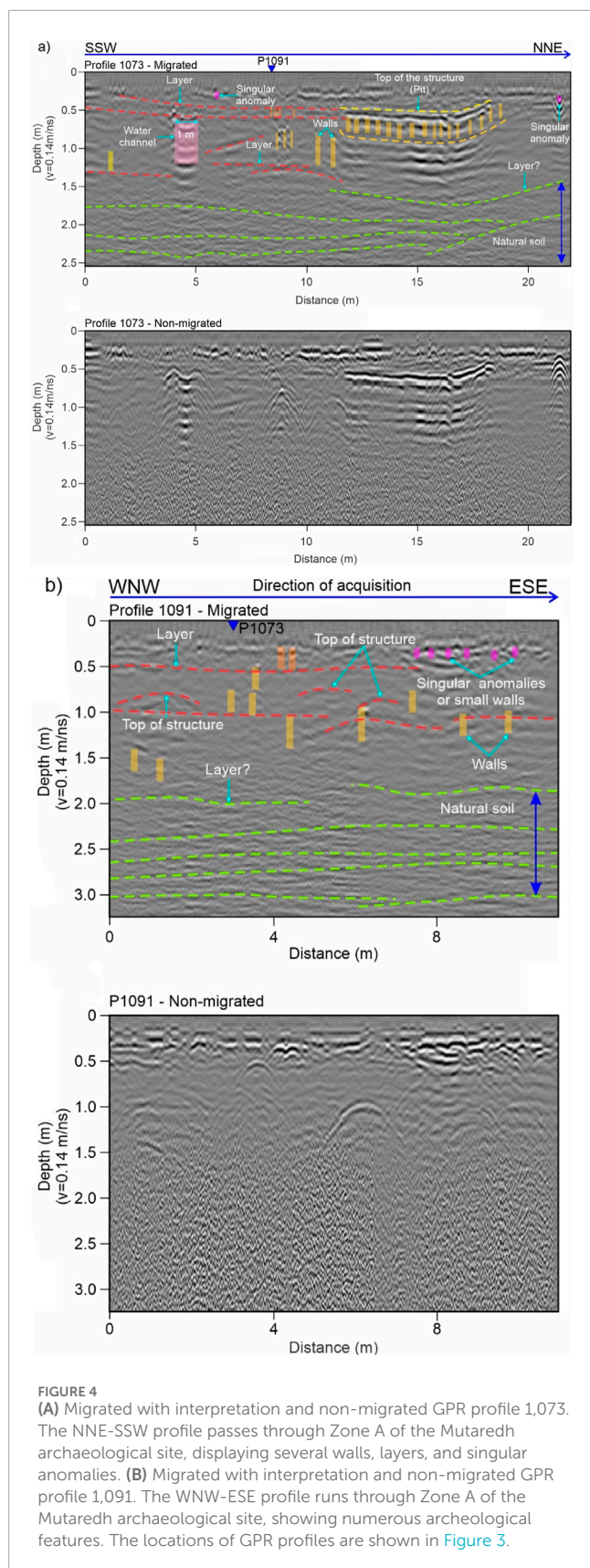|	
Samples	1,001
Signal position (ns)	2.916667
Distance interval (m)	0.017301
Time window (ns)	208.541667
Antenna separation (m)	0.330

3 Data processing

The acquired data underwent processing in the GPR Slice software through a series of sequential steps to enhance its quality. These steps included (1) Cropping the surface wave from the radar profiles in order to determine the time-zero of the radargram (Jol, 2008; Rasol et al., 2018), (2) Removing the average background values across scans on the horizontal axis, and (3) Applying a band-pass filter with a low cut-off at 264 MHz and a high cut-off at 1970 MHz (Neto and de Medeiros, 2006). The 264 MHz cut-off removed low-frequency noise from an unknown source, which was affecting the visualization of anomalies located at depths greater than 1.5 m. The high cut-off filter, set at 1970 MHz, removed high-frequency noise at a depth of 0.1 m, which obscured important shallow objects situated at this specific depth.

The next step involved applying gain to further enhance the imaging of deeper targets. In this case, manual adjustments were made to restore the energy loss in a specific layer (Maruddani and Sandi, 2019). The soil exhibited a distinct layer of fine materials, probably with higher clay content, where energy attenuation was pronounced. The last step was migration (5), a process that leads to the collapse of the energy into the source, allowing for accurate determination of the target's dimensions.

The velocity of the medium serves as an essential input for the migration. It was determined through hyperbola fitting (Dean et al., 2004; Conyers, 2015). A mean velocity of 0.14 m/ns proved effective in accurately migrating the sections, as most of the hyperbolae collapsed into the source of the energy. It is worth noting that the migration is performed in 2D, and analysis in this dimension alone is insufficient for a comprehensive understanding of the geometry of the encountered targets. Subsequently, the migrated data are sliced into 0.12 m thick blocks. This is crucial for analyzing the variability of the reflection amplitude in depth. To enhance the highest definition of the geometry in the horizontal plane parallel to the surface, a time slice, gridding is employed. This process involves a 0.05 m grid cell with a search radius of 0.5 m in both the x and y directions. The time slice is converted into a depth slice using an average velocity (0.14 m/ns). The identification of key anomalies within the depth slices guides the plotting of the 3D model. The method involves determining the thickness of a given anomaly by identifying its top and bottom slices. To plot the 3D structure, a vertical range (in nanoseconds) is selected, encompassing both

FIGURE 4
(A) Migrated with interpretation and non-migrated GPR profile 1,073. The NNE-SSW profile passes through Zone A of the Mutaredh archaeological site, displaying several walls, layers, and singular anomalies. (B) Migrated with interpretation and non-migrated GPR profile 1,091. The WNW-ESE profile runs through Zone A of the Mutaredh archaeological site, showing numerous archeological features. The locations of GPR profiles are shown in Figure 3.

the top and bottom slices. Next, a reflection amplitude range is chosen—typically around 20% of the highest amplitude values. This amplitude range creates a volume within the selected vertical range. The intersection of this volume with the time slice should align with the anomaly. If the volume exceeds the anomaly in the depth slice, the amplitude percentage should be reduced until it accurately matches the anomaly's area.

4 Results

The initial step in GPR interpretation involves a 2D analysis. In this context, understanding the geometry of many targets, especially non-linear ones, proves challenging when examining vertical sections. Linear objects appear consistently across parallel radargrams. However, the 2D investigation is valuable for mapping internal sub-structures, such as the location and diameter of inner walls or the presence of smaller trenches. Extracting such details can be complex or, at times, impossible from a 3D model.

Five representative GPR profiles have been interpreted to identify the primary archaeological features within the unexcavated region of the Mutaredh site (Figures 4, 5). This interpretation relies on pattern recognition, considering the geometry and extension of anomalies. It is crucial to note that the accuracy of measuring certain widths, such as the width of a wall, is only reliable when the profile crosses perpendicular (90°) to the structure. When crossing diagonally, the measured width will be significantly (and falsely) higher, especially as the angle between the profile and the structure decreases. In the extreme case where the profile is parallel to the structure, the hyperbola is converted into a flat and horizontal layer.
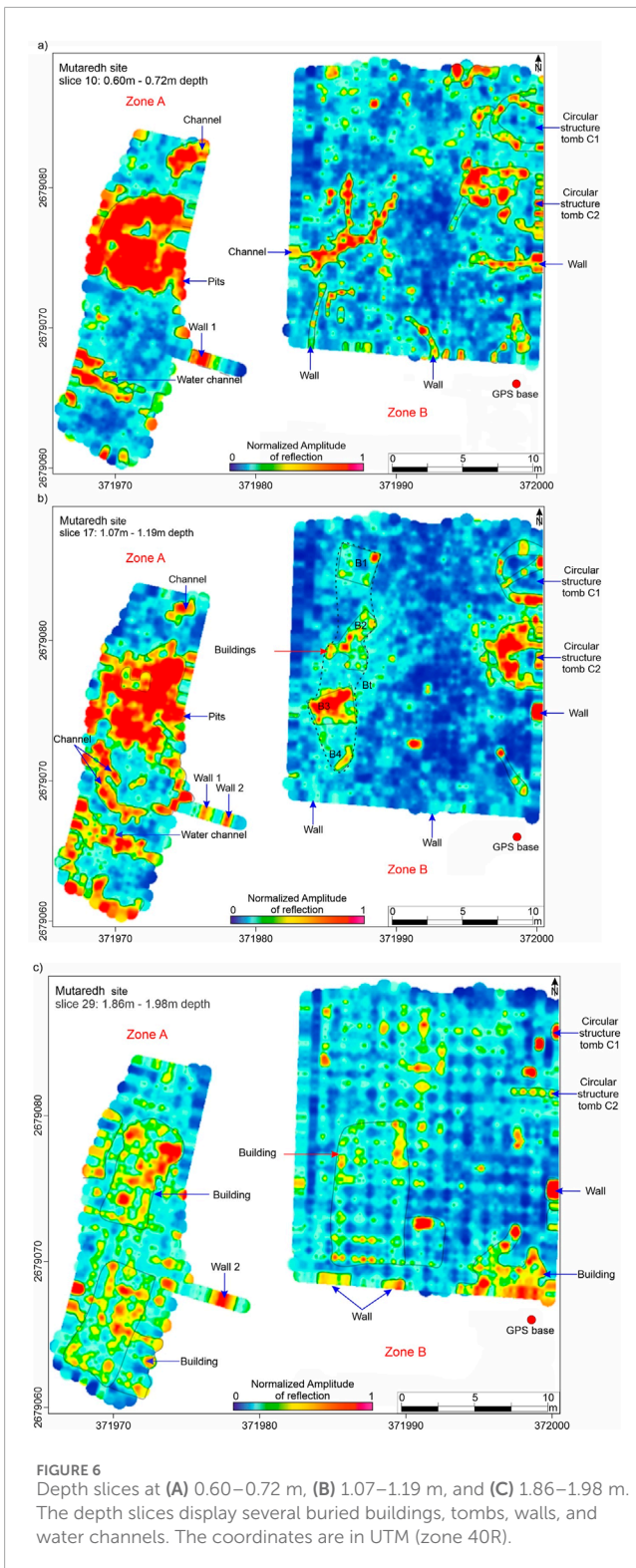
Profile 1,073 (Figure 4A) is situated in the unexplored Zone A with a total length of 22 m, adjacent to the previously excavated area (Figure 3), where the elements have already been categorized based on their usage and age. This profile runs perpendicular to profile 1,091 (Figure 4A), intersecting at 8.4 m. The interpreted profile 1,073 reveals an anomaly on its southern side, approximately 4.5 m from the start point, with a width of 1.0 m. The top of this structure is found at a depth of 0.55 m (Figure 4A). It is important to note that these values, both the depth and width of the anomaly, exhibit slight variations from profile to profile. Moreover, a 7 m wide structure is observed on the northern side of the profile, the top of which is detected at a depth of 0.5 m. Additionally, 0.5 m equispaced smaller hyperbolae are identified just beneath its top, indicating that the profile is perpendicular to inner elements (Figure 4A). In Profile 1,073, two sets of layers have been identified: those marked in red represent depths less than 1.5 m, while those in light green indicate deeper structures (>1.5 m). A few singular anomalies, and probably walls, have been observed at depths ranging from 0.25 to 2.25 m (Figure 4A). The WNW-ESE oriented Profile 1,091 intersects with Profile 1,073 at a horizontal distance of 3.2 m, crossing the discontinuity of the uncovered wall (D1, Figure 3). Several anomalies of interest are observed on the eastern side of the radargram. Singular
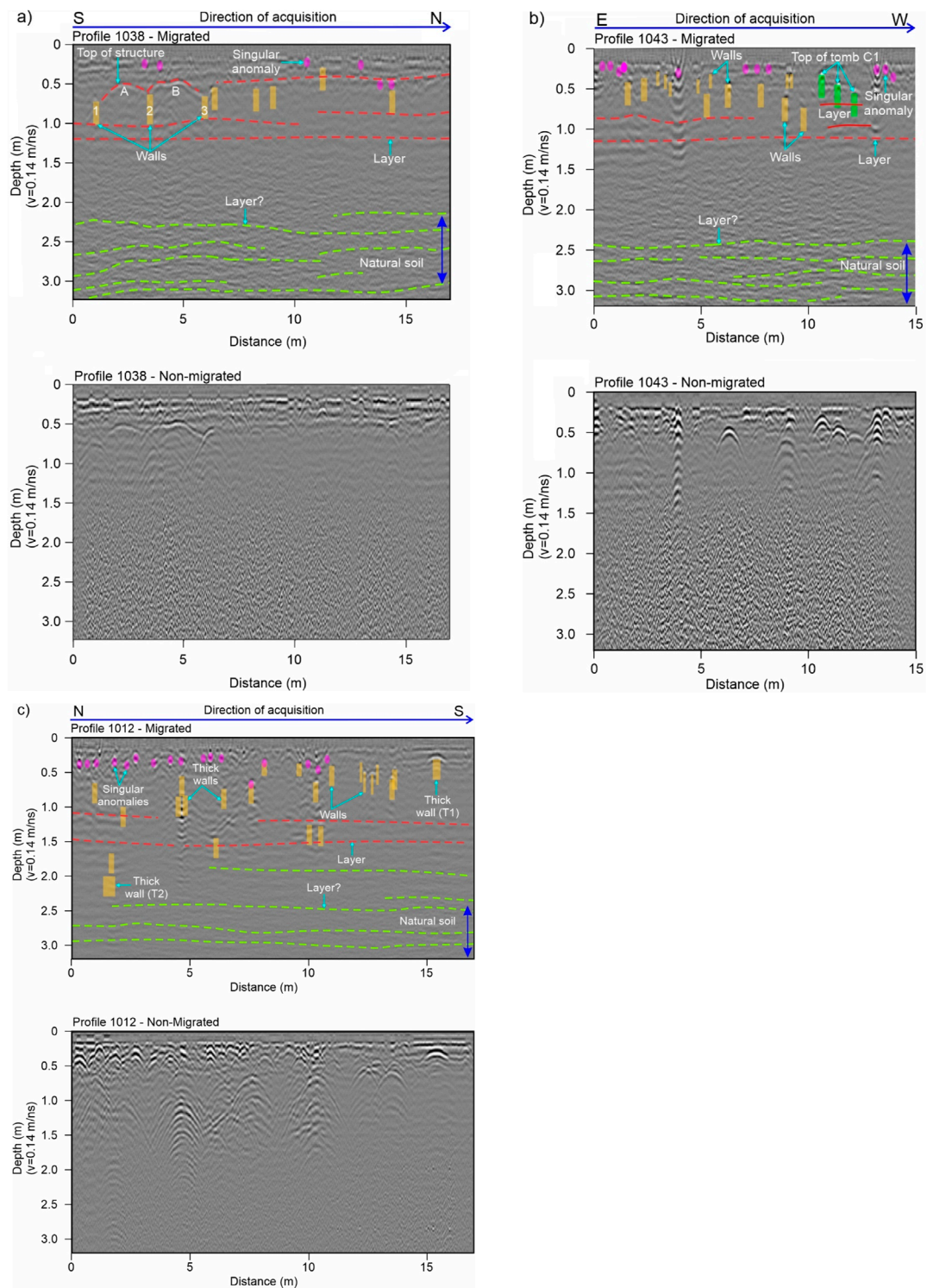
FIGURE 5
(A) Migrated with interpretation and non-migrated GPR profile 1038. The S-N profile cuts through the western part of Zone B of the Mutaredh archaeological site, revealing several archeological features. (B) Migrated with interpretation and non-migrated GPR profile 1043. The E-W profile, traversing the northern part of Zone B of the Mutaredh archaeological site, illustrates a tomb, walls, layers, and several singular anomalies. (C) Migrated with interpretation and non-migrated GPR profile 1012. The N-S profile cuts through the easternmost part of the Mutaredh archaeological site. The profile highlights several archeological features. The locations of the GPR profiles are shown in Figure 3.

anomalies at a depth of 0.25 m have been identified between 7.8 and 11 m horizontal distance, and they are most probably related to a structure rather than debris (Figure 4B). Similar to

what was observed in profile 1,073, numerous anomalies, likely walls, and both shallow and deeper layers (2–3 m) are found in Zone A (Figure 4B).

FIGURE 6
Depth slices at **(A)** 0.60−0.72 m, **(B)** 1.07−1.19 m, and **(C)** 1.86−1.98 m. The depth slices display several buried buildings, tombs, walls, and water channels. The coordinates are in UTM (zone 40R).

In the unexplored Zone B of the Mutaredh site, three GPR profiles have been interpreted to identify archeological features. Profiles 1,038 and 1,012 image the western and eastern ends of Zone B, respectively, while Profile 1,043 covers the northernmost part (Figures 3, 5). The N-S GPR profile 1,038 illustrates two individual structures (A and B) or segments of one structure (Figure 5A).

These features are located at a depth of 0.5 m, with the A structure measuring approximately 1.75 m, while the B structure measuring 1.5 m wide. Clear hyperbolae define the beginning (1), middle (2), and end (3) of the structure, suggesting the possibility of walls or the structure having sharp and abrupt geometry at its start and end. Additionally, wide hyperbolae located north of the A and B structures have been observed and may indicate the presence of additional walls. Moreover, numerous nearly flat and continuous layers are identified at shallow depths ranging from 0.5 to 1.2 m, as well as at deeper levels extending from 2 to 3.2 m (Figure 5A).
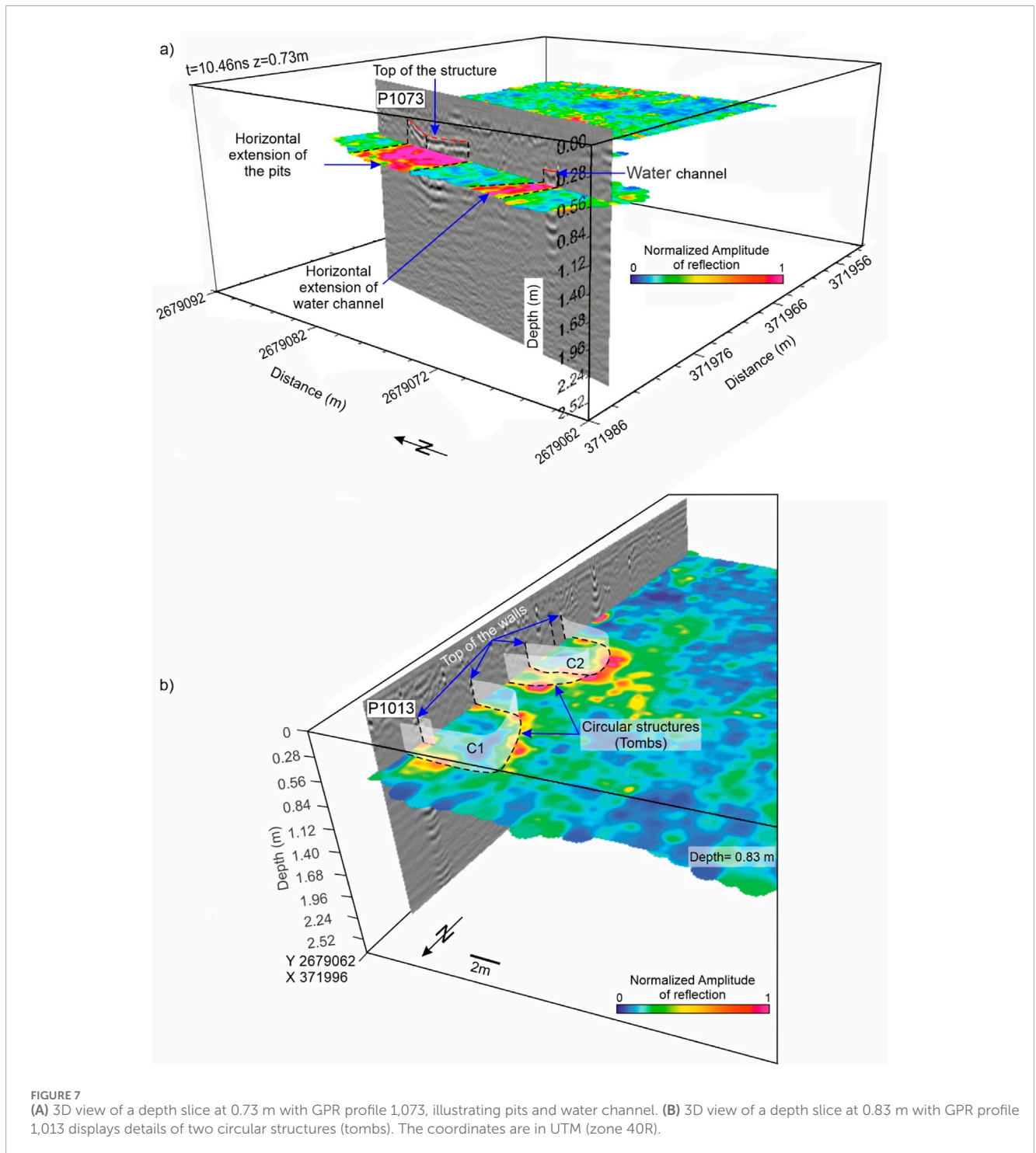
On the western side of Profile 1,043, shown in Figure 5B, multiple hyperbolae have been observed that are probably related to the top of a structure. Furthermore, numerous singular anomalies scattered throughout the profile are identified, possibly resulting from the deterioration of existing structures or even normal erosion of the surrounding limestone (Figure 5B). Similar features have been found in N-S Profile 1,012 (Figure 5C). Both profiles reveal various archeological features, including walls and nearly flat layers at different depths (Figures 5B, C). In Profile 1,012, at 15 m horizontal distance and 0.25 m depth, an important feature (T1) stands out, potentially related to a thicker wall compared to smaller anomalies (Figure 5C). Another wide hyperbola (T2) at a depth of 2.0 and 2 m horizontal distance from the profile's beginning suggests the presence of hidden archaeological remains (Figure 5C).

To generate a 3D volume, the migrated GPR data have been interpolated. The subsequent step involves slicing the volume into horizontal sections parallel to the surface. Three paradigmatic slices, selected from a total of 40 slices with a thickness of 0.12 m, have been extracted for a two-dimensional recognition of the main archaeological features in the Mutaredh site. The depth slices are as follows: slice 10 at 0.60−0.72 m, slice 17 at 1.07−1.19 m, and slice 29 at 1.86−1.98 m (Figure 6).

In Zone A of Mutaredh, slices 10 and 17 display similar anomalies, confirming a continuity between them. The first prominent feature is found in the southern part of Zone A. This anomaly is nearly linear, with a width varying between 1 and 1.5 m, extending horizontally at a bearing of 118° (Figures 6A, B). Its internal structure is visible on the southern side of Profile 1,073 (Figure 4A). Towards the north of this linear feature, a small feature has been observed at slice 10 (Figure 6A). However, at a deeper level in slice 17, two anomalies are identified (Figure 6B). They appear to run parallel to each other, oriented at 18° North (by the discontinuity D1 in Figure 3). The most substantial anomaly is located northwest of the uncovered walls, measuring approximately 7.5 m along the north-south axis and 7.2 m along the west-east axis at depth 0.6–0.72 m (Figure 6A). However, at depth 1.07–1.19 m, the anomaly exhibits higher definition and sharpness. Moreover, two anomalies west of the unearthed walls have been recognized, as well as a feature in the northernmost part and another anomaly in the southernmost part of Zone A (Figure 6B).

In Zone B, four agglomerations (B1, B2, B3, and B4) with higher amplitude of reflection are observed. The sizes of the anomalies are as follows (north-south x west-east): B1 is 2.5 m × 2.8 m, B2 is 4.5 m × 3 m, B3 is 2.5 m × 3.5 m, and B4 is 1.7 m × 1 m. The approximate area of Bt is 16 m × 4.5 m (Figures 6A, B). In the easternmost part of the Mutaredh site, two circular anomalies, labeled as C1 and C2, exhibit distinct characteristics. C1 has an outer diameter of 4.5 m and an inner diameter of 3.5 m (Figure 6B). On the other hand, C2 presents

FIGURE 7
(A) 3D view of a depth slice at 0.73 m with GPR profile 1,073, illustrating pits and water channel. (B) 3D view of a depth slice at 0.83 m with GPR profile 1,013 displays details of two circular structures (tombs). The coordinates are in UTM (zone 40R).

a more complex measurement challenge due to its irregular inner shape, with an outer diameter of 4.7 m and an inner diameter of approximately 2.5 m. It is plausible that C2 might be slightly deeper than C1, and the observed structure in this slice could be related to the top of the feature.

Figure 6C represents a deeper slice from 1.86 to 1.98 m. At this level, the signal-to-noise (SNR) ratio decreases, making distinguishing between buried targets and noisy signals challenging. In slice 29, the top view at this depth allows for identifying the

geometry of possible deep structures. However, the interpretation at this depth has higher uncertainty than slices 10 and 17 (Figure 6).

To interpret the anomaly effectively, it is necessary to intersect the slice with a vertical GPR profile of interest, allowing for visualization of continuity in both vertical and horizontal directions (Figure 7). Figure 7A provides a detailed intersection of profile 1,073 and the depth slice at 0.73 m. This intersection highlights two NW-SE anomalies in Zone A of the Mutaredh site. In Zone B, the intersection of profile 1,013 with a depth
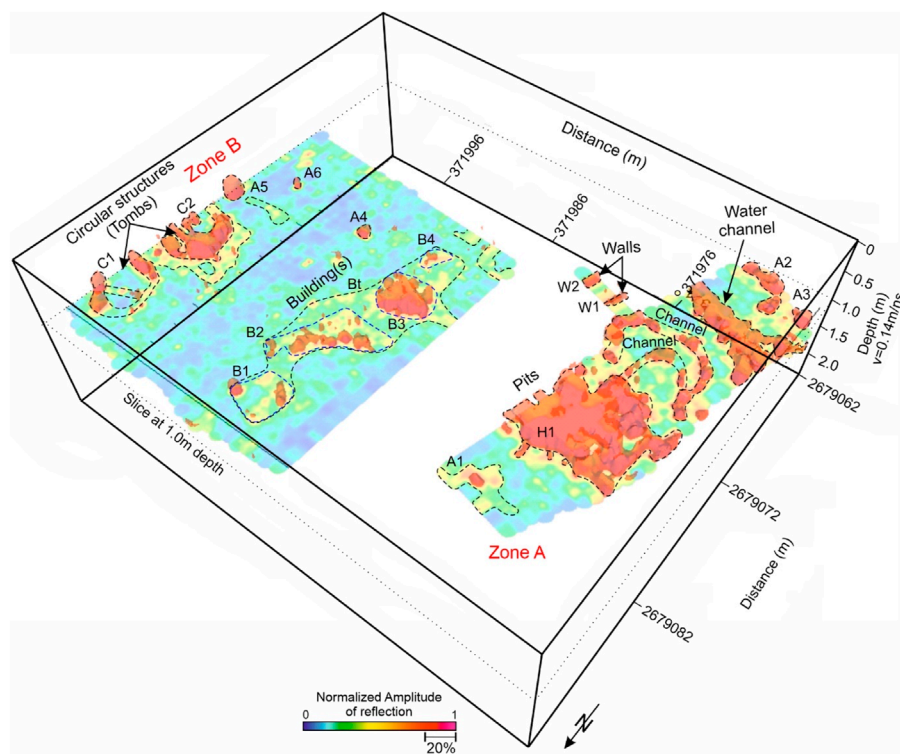
FIGURE 8
3D view of a depth slice at 1 m with plotting of the highest reflection amplitude (0.8–1). The view reveals two buried circular tombs, a building, and walls in Zone B, along with pits, water channels, and several walls (W1-W2) in Zone A of the Mutaredh archeological site. The coordinates are in UTM (zone 40R).

slice of 0.83 m illustrates two circular structures (C1 and C2). Both structures contain internal walls, suggesting divisions into sections or rooms (Figure 7B).

3D view of a depth slice at 1 m was extracted to visualize the geometry of the detected archeological features in a three-dimensional rendering image (Figure 8). The most significant anomalies are associated with the highest amplitude of reflection (0.8–1), where there is a notable contrast between the archeological materials (stone) and sand. To extract only the high amplitude reflections, only the top 20% of amplitudes are plotted (Figure 8). A time window ranging from 15 to 25 ns is defined to highlight key findings while disregarding very superficial small elements and deeper noisy signals. Despite certain areas not meeting the threshold for inclusion in the 20% highest amplitude range, evaluating the horizontal continuity of the slice at 1 m remains essential for perceiving the shape, extension, and orientation of features. This 3D view reveals a yellow area surrounding structures from B1 to B4 (not visible in slice 17, as shown in Figure 6B). This yellow area could represent the horizontal extension of these structures up to a maximum size denoted as Bt, indicating a higher degree of deterioration or possibly non-compacted soil compared to the outer part of Bt (Figure 8).

Some anomalies (A1-A6) remain unclassified or unlinked to nearby features. These anomalies are typically small and exhibit irregular and non-relatable geometries. For instance, A1's association with a wall is uncertain due to either significant

decay or the surrounding reflection amplitude (Figure 8). A2 might belong to a structure located in the southernmost part of Zone A, possibly connected to A3, with its size suggesting similarity to A2. Meanwhile, A4 and A6 stand isolated, making it challenging to connect them to any nearby archeological features; they could represent parts of walls, small pillars, or other structural elements. Conversely, A5 may be linked to the circular structures on the easternmost side of the Mutaredh site, particularly possibly connected to the feature C2 (Figure 8).

5 Discussion

The ground conditions at the Mutaredh archeological site are optimal for utilizing GPR to identify archaeological remnants. The sand in this area allows electromagnetic waves to pass through effectively, resulting in sharply defined subsurface targets at a penetration depth of 2.5 m. The SNR at values greater than 2.5 m depth is notably low, making it impossible to image any anomalies.

Several archaeological features have been identified on the acquired GPR profiles at various depths, likely corresponding to different historical periods. Consequently, these features are categorized into three distinct ages based on their geometry and depths: the Bronze Era, the Iron Age, and the Islamic Era. The shallower anomalies are potentially linked to the Islamic Era, while deeper anomalies are associated with the Bronze and Iron Ages. This
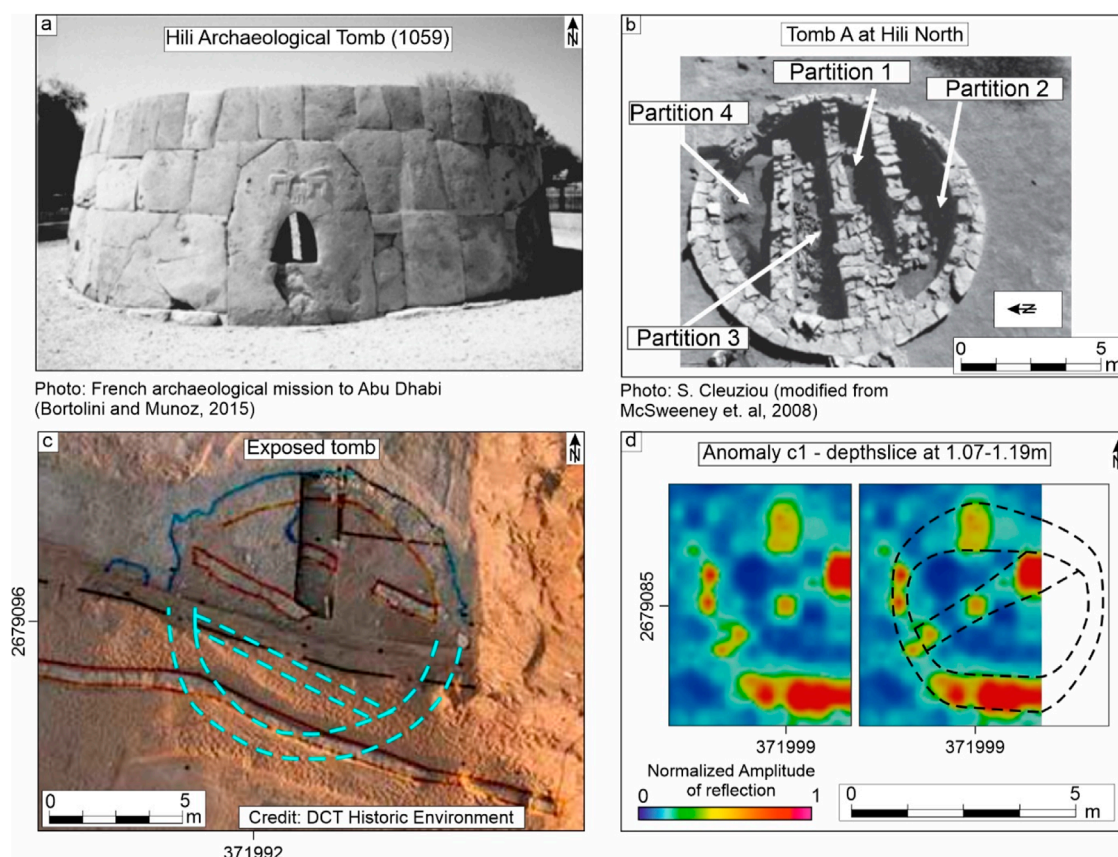
FIGURE 9
(A) Section view of Tomb 1,059 in the Hili Archaeological Park (after Bortolini and Munoz, 2015). **(B)** Top view of Tomb A in the Hili Archaeological Park (modified from McSweeney et al., 2008). **(C)** Top view of the unearthed tomb in the northeastern part of the Mutaredh site. **(D)** Top view of Tomb C1 identified by GPR data in the eastern part of the Mutaredh site. All tombs share a similar structural arrangement. The coordinates are in UTM (zone 40R).
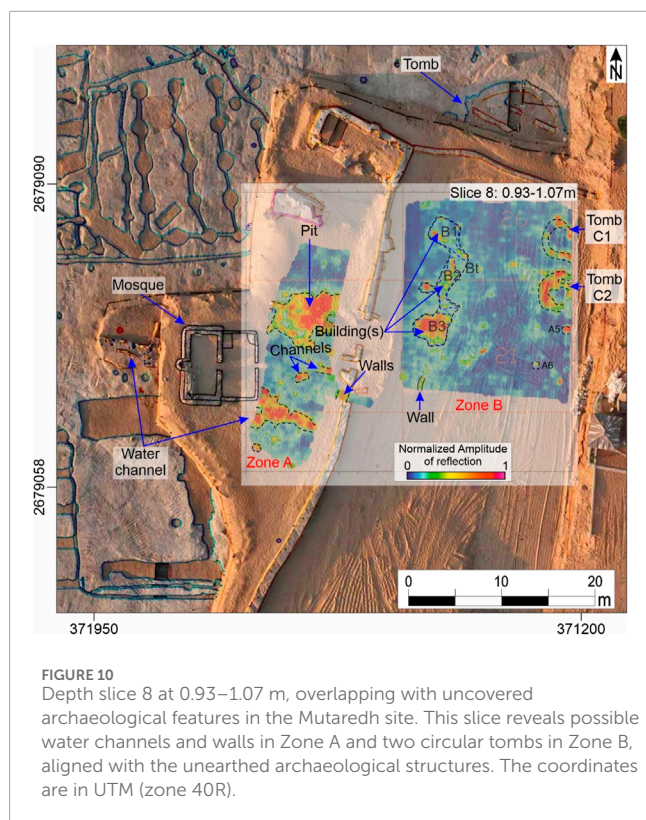
categorization is not solely based on depth but also characteristic features; for instance, circular tombs emblematic of the Bronze Age, while Mosques indicate the Islamic Era. Another factor aiding detection is the contrast between materials: limestone, predominant in structures and elements, contrasts with the dry reddish sand comprising the surrounding medium.

5.1 Bronze Age

Two circular structures were identified in the easternmost part of Mutaredh (Zone B) (Figures 5B, 7B, 8). Due to their geometry and larger diameters in deeper slices, these structures are likely tombs. A few meters to the north, archaeologists uncovered the northern half of a 12-m-diameter tomb (Figures 1C, 9; Sheehan, in press), dating to the Umm an-Nar period (2,700–2,000 BCE) of the Bronze Age. This dating is supported by fine pottery wares associated with funerary contexts and human bone remains (Sheehan, in press). The tombs identified by GPR are similarly likely from the Bronze Age, with diameters of approximately 4.5 m for Tomb C1 and 4.7 m for Tomb C2 (Figures 6, 10). Some internal features of these structures resemble those of the exposed tomb in the northeastern part of Mutaredh, and the circular Tomb 1,059 and North Tomb A at Hili

Archaeological Park (Figure 9; Cleuziou et al., 2011; Sheehan, in press). Tomb C1 features a diagonal wall oriented 45° north with a minimum thickness of 0.5 m, while Tomb C2 has a different internal layout, with walls oriented west-east (Figures 6B, 8, 9, 10). This discrepancy could suggest variations in the structural arrangement of the burial buildings or perhaps a similar layout with greater deterioration. Debris from partial collapses near the internal walls might create the illusion of thicker walls, as GPR cannot distinguish between solid walls and debris, which could also cause irregular shapes, such as protuberances extending from the main circular outline (Figures 6, 8).

Considering the potential dating of these structures to the Bronze Age, it is possible that deeper structures detected at 2.0 m or more buried beneath these tombs could predate them due to the natural sequence of superposition. Alternatively, these deeper anomalies may simply represent natural soil formations. The final depth slice, as shown in Figure 6C, suggests the presence of rectangular anomalies, although confirming this hypothesis is challenging due to the low SNR. Additionally, several singular, smaller, and irregularly sized anomalies could not be directly linked to known structures. However, their sizes indicate they could be related to debris from collapsed nearby features or even associated with everyday large-size tools such as pottery.

FIGURE 10
Depth slice 8 at 0.93–1.07 m, overlapping with uncovered archaeological features in the Mutaredh site. This slice reveals possible water channels and walls in Zone A and two circular tombs in Zone B, aligned with the unearthed archaeological structures. The coordinates are in UTM (zone 40R).

5.2 Iron Age

In the excavated western part of the Mutaredh site, archaeologists identified an array of cut features representing a complex system of irrigation channels and related tree pits (Figures 1C, 2A; Sheehan *P* in press). These irrigation channels, part of an agricultural complex, date back to Iron Age II (1,100–600 BCE). This association is supported by pottery found near the channels and a C14 date from burnt stones discovered in the pits (Sheehan, in press). The expected orientation, position, and width of these channels are aligned with those determined in the GPR results (Figures 6, 8, 10). Similar structures of comparable width have been detected in Al Ain (Tikriti, 2002; Wilkinson, 2002; Brook and Al Houqani, 2006; Alsharhan and Rizk, 2020). Another pronounced type of structure identified are potential tree pits of an agricultural system located at a depth of 0.5 m (Figures 4A, 6, 7A, 8, 10). These anomalies are probably internal pits (Figure 4A). Moreover, in the northernmost part of Zone A, an anomaly measuring 1.5 m in width and oriented at an angle of 63° North has been identified. This feature has been confirmed to be a water channel, as it shares the same width and orientation as the channel exposed during the archaeological excavation to the west of the survey area (Figures 6, 8, 10).

Furthermore, in Zone B of the Mutaredh site, an individual anomaly labeled as Bt appears to be associated with either a single building (divided into four spaces (B1 to B4) or four separate structures, the purposes of which remain unknown (Figures 6B, 8, 10). Furthermore, within each acquired radargram, singular anomalies were identified, which could be associated with small objects like pottery or other everyday items, likely related to the

Islamic or Iron civilizations in the Mutaredh site. These anomalies may also be linked to debris, including the visible small stones observed on the surface, resulting from the partial collapse of a structure due to natural deterioration and aging processes (Figures 4, 5).
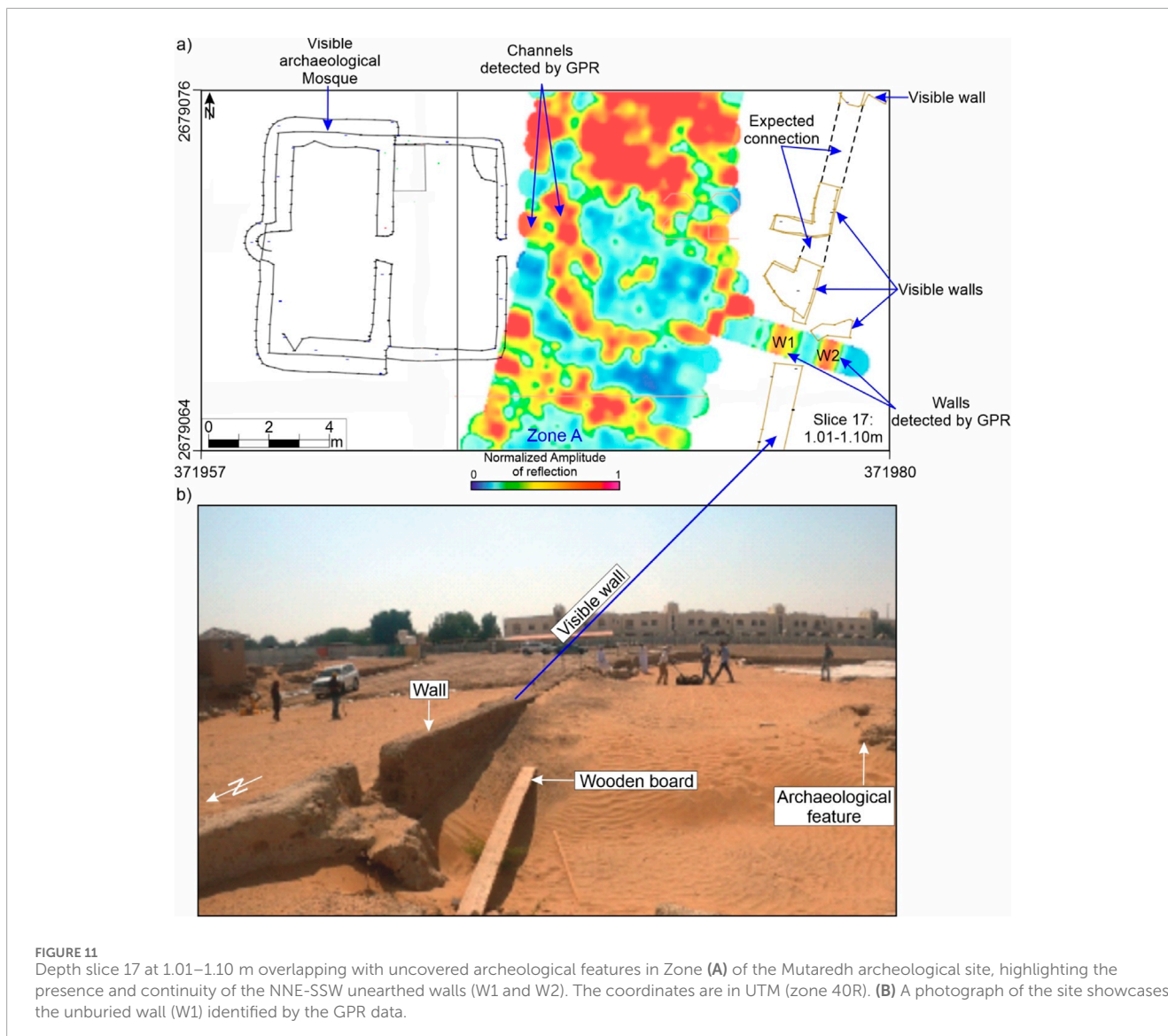
5.3 Late Islamic era

Despite the discovery of a mosque measuring 8.5 m in length and 7.6 m in width above the pre-BCE elements in the excavated western area of Mutaredh (Figure 1C), no evidence has been found for any Islamic buildings in the surveyed area (Zone A and Zone B). However, lengthy archaeological walls were uncovered, displaying several points of discontinuity (Figure 11). The exposed walls are likely related to agricultural field boundaries from the Late Islamic period (1,500–1,900 CE). This dating is based on the near-surface foundations found on the sand dunes and the construction materials, which resemble those of the nearby House of Ahmed Bin Suroor, excavated by DCT in 2005 (Sheehan, in press). A GPR profile conducted along one of the discontinuities (D1) successfully identified the same structure at the identical position both *in situ* and during post-processing analysis (W1; Figures 4B, 6A, 10, 11). Further investigation at a deeper level revealed the presence of either two distinct walls or a single, thicker one (Figures 6B, 11A). These were measured to be 1 m wide for the west wall (W1) and 0.75 m wide for the east wall (W2), within a depth slice ranging from 1.07 to 1.19 m. This specific profile (1,091) serves to confirm the accuracy and precision of both the GPR survey and GPS positioning (Figure 4A). Moreover, within each acquired radargram, singular anomalies were identified, which could be associated with small objects like pottery or other everyday items, likely related to the Islamic civilization in Mutaredh site. These anomalies may also be linked to debris, including the visible small stones observed on the surface, resulting from the partial collapse of a structure due to natural deterioration and aging processes (Figures 4, 5).

6 Conclusion

The high-resolution GPR survey conducted in this study has provided insightful subsurface and non-invasive imaging of the Mutaredh archaeological site in Al Ain. The distinct contrast between construction materials, typically limestone, and the surrounding reddish dry sand has enabled clear and, in some instances, sharp imaging of buried structures up to a depth of 2.0 m. However, interpretation of deeper anomalies, particularly those between 2.0 and 2.5 m, was made with less confidence. Beyond this depth, no further elements could be detected due to reduced signal clarity and natural energy decay.

Based on GPR interpretation, two circular features are aligned with the unearthed Bronze Age tomb located in the northeastern part of the Mutaredh site, suggesting the presence of smaller tombs with a similar layout. Furthermore, several significant archaeological findings have been documented at the site, proving the continuity of an exposed water channel system that could be linked to a *falaj* channel, the discovery of extensive features forming part of a complex agricultural system, and the observation of four individual

FIGURE 11
Depth slice 17 at 1.01–1.10 m overlapping with uncovered archeological features in Zone **(A)** of the Mutaredh archeological site, highlighting the presence and continuity of the NNE-SSW unearthed walls (W1 and W2). The coordinates are in UTM (zone 40R). **(B)** A photograph of the site showcases the unburied wall (W1) identified by the GPR data.

structures or sections within a larger structure, possibly serving as small houses or storage units. These archaeological features are interpreted to be related to the Iron Age. The features identified as walls likely belong to the Late Islamic period. Their location and orientation align with the uncovered Islamic walls at the Mutaredh site. Numerous shallow singular anomalies, possibly related to daily tools or debris resulting from structural deterioration, were observed and may similarly be associated with the Late Islamic Period. The density, quantity, and size of detected elements suggest intensive site habitation across different historical periods, including the Bronze and Iron Ages and the Late Islamic period. Nevertheless, further verification and ground-truthing through excavation is necessary to validate interpretations regarding characterization and depth. The findings of this work can serve as guidance for archaeologists during the ground-truthing phase in the Mutaredh site. Moreover, this case study demonstrates how buried tombs, water channels, and walls are interpreted through radargrams and 3D models. These findings may aid in pattern recognition for future surveys.

Data availability statement

The raw data supporting the conclusions of this article will be made available by the authors, without undue reservation.

Author contributions

SS-A: Conceptualization, Data curation, Formal Analysis, Investigation, Methodology, Visualization, Writing–original draft, Writing–review and editing. MA: Data curation, Formal Analysis, Methodology, Software, Visualization, Writing–original draft, Writing–review and editing. MYA: Project administration,

Resources, Supervision, Validation, Writing–review and editing. DF: Formal Analysis, Funding acquisition, Project administration, Supervision, Validation, Writing–review and editing. PS: Investigation, Resources, Validation, Writing–review and editing. WO: Methodology, Resources, Writing–review and editing. MI: Data curation, Software, Writing–review and editing.

Funding

Acknowledgments

Conflict of interest

The authors declare that the research was conducted in the absence of any commercial or financial relationships that could be construed as a potential conflict of interest.

The author(s) declared that they were an editorial board member of Frontiers, at the time of submission. This had no impact on the peer review process and the final decision.

Publisher's note

All claims expressed in this article are solely those of the authors and do not necessarily represent those of their affiliated organizations, or those of the publisher, the editors and the reviewers. Any product that may be evaluated in this article, or claim that may be made by its manufacturer, is not guaranteed or endorsed by the publisher.

References

Ali, M. Y., Sirat, M., and Small, J. (2008). Geophysical investigation of Al Jaww Plain, eastern Abu Dhabi: implications for structure and evolution of the frontal fold belts of the Oman Mountains. *GeoArabia* 13 (2), 91–118. doi:10.2113/geoarabia130291

Al Marzooqi, N. N., Sheehan, P., Power, T., and Al Ajou, M. (2024). "New evidence for the early islamic landscape of Al Ain fieldwalking and surface ceramics from slemi, jimi region," in Advances in UAE archaeology: proceedings of Abu dhabi's archaeology conference 2022. Archaeopress Publishing Ltd, 377.

Alnimee, A. (2020). The protection of archeological sites in the United Arab Emirates law. *Alrafidain Law* 22 (71), 101–129.

Al-Ruzouq, R., Abu Dabous, S., Abueladas, A., Hosny, F., and Ibrahim, F. (2022). Integrated archaeological modeling based on geomatics techniques and ground-penetrating radar. *Remote Sens.* 14 (7), 1622. doi:10.3390/rs14071622

Alsharhan, A. S., and Rizk, Z. E. (2020). Aflaj systems: history and factors affecting recharge and discharge. *Water Resour. Integr. Manag. United Arab Emir.*, 257–280. doi:10.1007/978-3-030-31684-6_8

Al Tikriti, W., Omar, W. A., Al Tawalbeh, D. A., Al Nuaimi, A. R., Al Kaabi, A. K., et al. (2013). *Looking for tawam through the sand: geophysical investigations at oud Al toba, Al-Ain, UAE.* Second EAGE international conference on engineering geophysics. Al Ain, United Arab Emirates: European Association of Geoscientists and Engineers, pp. cp-368.

Al-Tikriti, W., Al-Neyadi, M., Tawalbeh, D., Al-Nuaimi, A. R., Al-Kaabi, A., Omar, W., et al. (2015). *Filling a blank: new excavations at an early Islamic site at Oud Al Toba/Muataredh in al-ʿAyn, UAE.* Proceedings of the seminar for Arabian studies. London, United Kingdom: JSTOR, 371–384.

Annan, A. (2009). Electromagnetic principles of ground penetrating radar. *Ground penetrating radar theory Appl.* 1, 1–37. doi:10.1016/B978-0-444-53348-7.00001-6

Assunção, S. S., Arancibia, V. S., Gracia, V. P., et al. (2018). "Geophysical survey of an archaeological iberian village by means of ground penetrating radar," in 2018 17th international conference on ground penetrating radar (GPR). Switzerland: IEEE, 1–5.

Barbaro, G., Foti, G., Barillà, G. C., and Frega, F. (2022). Beach and dune erosion: causes and interventions, case study: kaulon archaeological site. *J. Mar. Sci. Eng.* 10 (1), 14. doi:10.3390/jmse10010014

Belmonte, J., and González-García, A. (2014). On the orientation of early bronze age tombs in ancient Magan. *Mediterr. Archaeol. Archaeom.* 14 (3), 233–246.

Ben-Romdhane, H., Francis, D., Cherif, C., Pavlopoulos, K., Ghedira, H., and Griffiths, S. (2023). Detecting and predicting archaeological sites using remote sensing and machine learning—application to the saruq Al-hadid site, Dubai, UAE. *Geosciences* 13 (6), 179. doi:10.3390/geosciences13060179

Böhme, M., and Al-Sabri, B. A. (2011). Umm an-Nar burial 401 at bat, Oman: architecture and finds. *Arabian Archaeol. Epigr.* 22 (2), 113–154. doi:10.1111/j.1600-0471.2011.00341.x

Bortolini, E., and Munoz, O.(2015). "Life and death in prehistoric Oman: Insights from Late Neolithic and Early Bronze Age funerary practices (4th-3rd mill. BC)," in The Archaeological Heritage of Oman, Proceedings of the symposium held at UNESCO, September, 7th 2012. Ministry of Heritage and Culture, Sultanate of Oman; UNESCO, 61–80.

Brook, M., and Al Houqani, H. (2006). *Current status of aflaj in the Al Ain area. United Arab Emirates: United Arab Emirates.* Abu Dhabi: Environment Agency.

Bullock, E. C. (2013). *An archaeological/genealogical historical analysis of the National Council of Teachers of Mathematics' Standards documents.* United States of America: Georgia State University.

Büyüksaraç, A., Yalçıner, C. Ç., Ekinci, Y. L., Demirci, A., and Yücel, M. A. (2014). Geophysical investigations at agadere cemetery, Gallipoli Peninsular, NW Turkey. *Aust. J. Forensic Sci.* 46 (1), 111–123. doi:10.1080/00450618.2013.804948

Caratelli, P., Misuri, M. A., and El Amrousi, M. (2019). Al-Ain's cultural landscape: identity, innovation and sustainability in a challenging economy. *Int. Rev. spatial Plan. Sustain. Dev.* 7 (3), 45–62. doi:10.14246/irspsda.7.3_45

Carbó, A., Córdoba, J., Muñoz, A., and Ramos, P. (2000). "*Retrieving the life of the Iron age archaeological excavations and geophysical survey at Al-Madam (UAE Sharjah) impressions after the 1999 season,*" in Proceedings of the seminar for arabian studies. Brepols. London, United Kingdom: JSTOR, 61–68.

Carter, R. (1997). "*The Wadi Suq period in south-east Arabia: a reappraisal in the light of excavations at Kalba, UAE,*" in Proceedings of the seminar for arabian studies. JSTOR.

Cherif, O. H., Al-Rifaiy, I. A., and El-Deeb, W. Z. M. (1992). *Post-napes early tertiary foraminiferal paleoecology of the northern Hafit area, south of Al-Ain city (United Arab Emirates).* Micropaleontology 38, 37–56.

Cleuziou, S. (2003). "*Early bronze age trade in the Gulf and the arabian sea: the society behind the boats,*" in Archaeology of the United Arab Emirates: proceedings of the first international conference on the archaeology of the UAE. London: Trident Press.

Cleuziou, S., Méry, S., and Vogt, B. (2011). *Protohistoire de l'oasis d'al-Aïn, travaux de la mission archéologique française à Abou Dhabi (Emirats arabes unis): les sépultures de l'âge du Bronze.* Archaeopress.

Conyers, L. B. (2007). "Ground-penetrating radar for archaeological mapping," in *Remote sensing in archaeology.* Springer, 329–344.

Conyers, L. B. (2015). Analysis and interpretation of GPR datasets for integrated archaeological mapping. *Near Surf. Geophys.* 13 (6), 645–651. doi:10.3997/1873-0604.2015018

Conyers, L. B. (2023). *Ground-penetrating radar for archaeology*. Washington DC, United States of America: Rowman and Littlefield.

Daniels, D. (2004). *Ground penetrating radar*, in The institution of engineering and technology publishing.

Daniels, J. J. (2000). *Ground penetrating radar fundamentals*, 1–21. Prepared as an appendix to a Report to the US EPA, Region V.

Dean, G., Yasushi, N., Kent, S., Salvadore, P., Hiromichi, H., and Noriaki, H. (2004). Advances in imaging of subsurface archaeology using GPR. *Journal of the Korean Geophysical Society* 7 (3). 161–170.

El-Qady, G., and Metwaly, M. (2019). "Geophysical techniques applied in archaeology," in *Archaeogeophysics: state of the art and case studies*. Springer, 1–25.

Evangelista, R., Magee, P., and Wedepohl, E. (2002). 3D imaging of an Iron Age archaeological site: GPR analysis at Muweilah, United Arab Emirates(UAE), in Ninth international conference on ground penetrating radar. SPIE 4758, 1O8–114.

Fahmy, A., Domínguez-Bella, S., Martínez-López, J., and Molina-Piernas, E. (2023). Sand dune movement and flooding risk analysis for the pyramids of Meroe, Al Bagrawiya archaeological site, Sudan. *Herit. Sci.* 11 (1), 136. doi:10.1186/s40494-023-00986-5

Frifelt, K. (1991). The island of Umm an-Nar/1 Third millennium graves. *Jysk Arkæol. Selsk*.

Gabler, M., Trinks, I., Nau, E., Hinterleitner, A., Paasche, K., Gustavsen, L., et al. (2019). Archaeological prospection with motorised multichannel ground-penetrating radar arrays on snow-covered areas in Norway. *Remote Sens.* 11 (21), 2485. doi:10.3390/rs11212485

Gaffney, C. (2008). Detecting trends in the prediction of the buried past: a review of geophysical techniques in archaeology. *Archaeometry* 50 (2), 313–336. doi:10.1111/j.1475-4754.2008.00388.x

Giardino, C. (2017). *Magan—the land of copper: prehistoric metallurgy of Oman the archaeological heritage of Oman, 2*. Oxford, United Kingdom: Ministry of Heritage and Culture of the Sultanate of Oman. Archaeopress Publishing.

Goodman, D., and Piro, S. (2013). *GPR remote sensing in archaeology*. Springer.

Herrmann, J. T. (2013). Three-dimensional mapping of archaeological and sedimentary deposits with ground-penetrating radar at saruq al-hadid, Dubai, United Arab Emirates. *Archaeol. Prospect.* 20 (3), 189–203. doi:10.1002/arp.1456

Hey, G. (2006). "Scale and archaeological evaluations: what are we looking for?," in *Confronting scale in archaeology: issues of theory and practice*. Springer, 113–127.

Hinze, W. J., Von Frese, R. R., Von Frese, R., and Saad, A. H. (2013). *Gravity and magnetic exploration: principles, practices, and applications*. Cambridge University Press.

James Blackman, M., Mery, S., and Wright, R. P. (1989). Production and exchange of ceramics on the Oman peninsula from the perspective of Hili. *J. Field Archaeol.* 16 (1), 61–77. doi:10.2307/529881

Jol, H. M. (2008). *Ground penetrating radar theory and applications*. Elsevier.

Jorgensen, D. G., and al-Tikiriti, W. Y. (2003). A hydrologic and archeologic study of climate change in Al Ain, United Arab Emirates. *Glob. Planet. Change* 35 (1-2), 37–49. doi:10.1016/s0921-8181(02)00090-5

Kearey, P., Brooks, M., and Hill, I. (2002). *An Introduction to Geophysical Exploration*. Oxford: Blackwell Science Ltd.

Kim, G., and Heliyer, P. (2003). Islamic archaeology in the deep sands of Abu Dhabi emirate, UAE. *Archaeol. United Arab Emir.* 264.

Koşaroğlu, S., Kamacı, Z., Erdoğan, S., Bektaş, Ö., and Büyüksaraç, A. (2022). Determination of historical graves by ground penetrating radar method: sakarya Field Battle (August 23–September 13, 1921, Turkey). *Aust. J. Forensic Sci.* 54 (6), 842–860. doi:10.1080/00450618.2021.1921270

Madsen, B. (2018). *The early Bronze age tombs of Jebel Hafit: Danish archaeological investigations in Abu Dhabi 1961-1971*. Demark: Aarhus Universitetsforlag.

Maruddani, B., and Sandi, E. (2019). The development of ground penetrating radar (GPR) data processing. *Int. J. Mach. Learn. Comput.* 9 (6), 768–773. doi:10.18178/ijmlc.2019.9.6.871

McManamon, F. P. (1984). "Discovering sites unseen," in *Advances in archaeological method and theory*. Elsevier, 223–292.

McSweeney, K., Méry, S., Negri, S., and Macchiarelli, R.(2008). Rewriting the end of the Early Bronze Age in the United Arab Emirates through the anthropological and artefactual evaluation of two collective Umm an-Nar graves at Hili (eastern region of Abu Dhabi). *Arabian archaeology and epigraphy* 19(1), 1–14.

MRMEWR (2011). "Ministry of regional municipalities, environment and water resources, sultanate of Oman," in *Aflaj inventory project summary report*.

Neto, P. X., and de Medeiros, W. E. (2006). A practical approach to correct attenuation effects in GPR data. *J. Appl. Geophys.* 59 (2), 140–151. doi:10.1016/j.jappgeo.2005.09.002

Neubauer, W., Eder-Hinterleitner, A., Seren, S., and Melichar, P. (2002). Georadar in the Roman civil town Carnuntum, Austria: an approach for archaeological interpretation of GPR data. *Archaeol. Prospect.* 9 (3), 135–156. doi:10.1002/arp.183

Nuzzo, L., Leucci, G., Negri, S., Carrozzo, M. T., and Quarta, T. (2002). Application of 3D visualization techniques in the analysis of GPR data for archaeology. *Ann. Geophys*. doi:10.4401/ag-3517

Palumbo, G., al-Tikriti, W. Y., Mahdy, H., al Nuaimi, A., al Kaabi, A., Altawallbeh, D. E., et al. (2014). Protecting the invisible: site-management planning at small archaeological sites in al-Ain, Abu Dhabi. *Conservation Manag. Archaeol. sites* 16 (2), 145–162. doi:10.1179/1350503314z.00000000079

Parcak, S. (2007). Satellite remote sensing methods for monitoring archaeological tells in the Middle East. *J. Field Archaeol.* 32 (1), 65–81. doi:10.1179/009346907791071773

Parcak, S., Gathings, D., Childs, C., Mumford, G., and Cline, E. (2016). Satellite evidence of archaeological site looting in Egypt: 2002–2013. *Antiquity* 90 (349), 188–205. doi:10.15184/aqy.2016.1

Pérez-Gracia, V., González-Drigo, R., and Sala, R. (2012). Ground-penetrating radar resolution in cultural heritage applications. *Near Surf. Geophys.* 10 (1), 77–87. doi:10.3997/1873-0604.2011015

Potts, D. T. (1993). The late prehistoric, protohistoric, and early historic periods in Eastern Arabia (ca. 5000–1200 BC). *J. World Prehistory* 7, 163–212. doi:10.1007/bf00975450

Potts, D. T. (2012). *In the land of the Emirates: the archaeology and history of UAE*. Abu Dhabi: Trident Press.

Power, T., Benoist, A., and Sheehan, P. (2019). An Iron age ceramic sequence from the bayt Bin ati, al-ain, UAE. *Arabian Archaeol. Epigr.* 30 (1), 75–102. doi:10.1111/aae.12122

Power, T., and Sheehan, P. (2012). The origin and development of the oasis landscape of al-ʿAin (UAE), in *Proceedings of the seminar for arabian studies*. JSTOR.

Raffaele, L., and Bruno, L. (2019). Windblown sand action on civil structures: definition and probabilistic modelling. *Eng. Struct.* 178, 88–101. doi:10.1016/j.engstruct.2018.10.017

Rasol, M., Pérez-Gracia, V., and Assunçao, S. S. (2018). Analysis and calibration of ground penetrating radar shielded antennas, in 2018 17th international conference on ground penetrating radar (GPR). IEEE, 1–4.

Reynolds, J. M. (2011). *An introduction to applied and environmental geophysics*. John Wiley and Sons.

Roumelioti, Z., Paraskevopoulos, P., Moustakas, H., Koilanitis, M., Sokos, E., Avramidis, P., et al. (2022). Detecting and mapping the buried past: GPR surveys at two archaeological sites in achaea, Greece.

Santos-Assunçao, S., Dimitriadis, K., Konstantakis, Y., Perez-Gracia, V., Anagnostopoulou, E., and Gonzalez-Drigo, R. (2016). Ground-penetrating radar evaluation of the ancient Mycenaean monument Tholos Acharnon tomb. *Near Surf. Geophys.* 14 (2), 197–205. doi:10.3997/1873-0604.2015030

Schiffer, M. B., Sullivan, A. P., and Klinger, T. C. (1978). The design of archaeological surveys. *World Archaeol.* 10 (1), 1–28. doi:10.1080/00438243.1978.9979712

Sheehan, P., Power, T., Kaabi, O. A., Khalifa, M., Al-Dhaheri, M., Al-Mansoori, B., et al. (2015). "*Rediscovering a 'lost' village of al-ʿAyn: archaeology and communal memory in the oasis (poster)*," in Proceedings of the seminar for arabian studies. London, United Kingdom: JSTOR.

Sheehan, P., Al Marzouqi, N. N., Khalifa, M., and Al Ajou, M. (2024). *Mutaredh Community Mall – more insights into the development of the hydraulic, agricultural and funerary landscapes of al-ʿAyn (UAE)*, in Proceedings of the seminar for arabian studies 53. London, United Kingdom: In press.

Strutt, K., Beech, M. J., Blue, L., and Sheehan, P. (2013). Archaeological and maritime surveys on the island of ghagha, Al gharbia, Abu Dhabi, United Arab Emirates. *ISAPNews Int. Soc. Archaeol. Prospect.* 35, 17–20.

Suryanarayan, A., Méry, S., Mazuy, A., and Regert, M. (2022). Foodstuffs and organic products in ancient SE Arabia: preliminary results of ceramic lipid residue analysis of vessels from Hili 8 and Hili North Tomb A, al Ain, United Arab Emirates, in *Proceedings of the seminar for arabian studies*.

Swerida, J. (2018). Bat and the Umm an-Nar settlement tradition, in *Beyond tombs and towers: domestic architecture of the Umm an Nar period in eastern Arabia*, 51–70.

Telford, W. M., Geldart, L. P., and Sheriff, R. E. (1990). *Applied geophysics*. United Kingdom: Cambridge University Press.

Tikriti, W. Y. A. (2002). The south-east Arabian origin of the falaj system, in *Proceedings of the seminar for arabian studies*. JSTOR.

Trinks, I., Johansson, B., Gustafsson, J., Emilsson, J., Friborg, J., Gustafsson, C., et al. (2010). Efficient, large-scale archaeological prospection using a true three-dimensional ground-penetrating radar array system. *Archaeol. Prospect.* 17 (3), 175–186. doi:10.1002/arp.381

Ullah, S., Ali, M. Y., Iqbal, M. A., Bouchaala, F., and Saibi, H. (2023). Structures and stratigraphy of Al Jaww Plain, southeastern Al Ain, United Arab Emirates: implications for aquifer systems and mantle thrust sheet. *Geosci. Lett.* 10 (1), 53. doi:10.1186/s40562-023-00308-4

Warrak, M. (1996). Origin of the Hafit structure: implications for timing the tertiary deformation in the northern Oman mountains. *J. Struct. Geol.* 18 (6), 803–818. doi:10.1016/s0191-8141(96)80014-9

White, A. P. (2013). X marks the spot: extracting data from historical maps to locate archaeological sites. *J. Map and Geogr. Libr.* 9 (1-2), 140–156. doi:10.1080/15420353.2013.767764

Wilkinson, J. (2002). The origins of the aflāj of Oman. *Prod. Exploitation Resour.* 285.

Yagoub, M., and Al Yammahi, A. A. (2022). Spatial distribution of natural hazards and their proximity to heritage sites: case of the United Arab Emirates. *Int. J. Disaster Risk Reduct.* 71, 102827. doi:10.1016/j.ijdrr.2022.102827